The 1-soliton in the $SO(3)$ gauged Skyrme model with mass term

Y. Brihaye$^{\diamond}$, J. Burzlaff‡*, V. Paturyan†, and D. H. Tchrakian†*

$^{\diamond}$Physique-Mathématique, Université de Mons-Hainaut, Mons, Belgium

‡School of Mathematical Sciences, Dublin City University, Dublin 9, Ireland

†Department of Mathematical Physics, National University of Ireland Maynooth, Maynooth, Ireland

*School of Theoretical Physics – DIAS, 10 Burlington Road, Dublin 4, Ireland

Abstract

The solitons of the $SO(3)$ gauged Skyrme model with no pion-mass potential were studied in Refs. [1, 2]. Here, the effects of the inclusion of this potential are studied. In contrast with the (ungauged) Skyrme model, where the effect of this potential on the solitons is marginal, here it turns out to be decisive, resulting in very different dependence of the energy as a function of the Skyrme coupling constant.

1 Introduction

The solitons of the $SO(3)$ gauged Skyrme model with no pion mass potential were studied in detail numerically in Refs. [1, 2]. The model

$$\mathcal{H}_0 = -\frac{1}{4}\text{Tr}|F_{ij}|^2 + \text{Tr}\left((U^{-1}D_iU)^2 + \kappa([U^{-1}D_iU, U^{-1}D_jU])^2\right) \tag{1}$$

was determined by the vector gauging prescription defined by the covariant derivative

$$D_iU = \partial_iU + [A_i, U] , \qquad U = \cos f + i\mathbf{n}.\boldsymbol{\sigma}\sin f , \tag{2}$$

where U is an element of $SU(2)$, and the (antihermitian) Yang-Mills connection and curvature are in the algebra.

Replacing ∂_iU in the usual Skyrme model [3] by (2) yields the model (1) studied in [1, 2]. In the present work, we augment this system $\mathcal{H}_0$ by the familiar pion-mass[1] potential

$$V = \lambda(1 - \cos f) \tag{3}$$

such that the system we study here is $\mathcal{H} = \mathcal{H}_0 + \lambda(1 - \cos f)$.

The effects of this, as we shall see from our numerical work in Section 3, are considerable, in contrast with the usual (ungauged) Skyrme model [3] where the only effect is the quantitative one of rendering the asymptotic decay exponential rather than power like.

We are interested in *unit* Baryon number solitons, hence only in spherically symmetric solutions. Imposition of spherical symmetry leads to

$$A_i = -\frac{i}{2}\left(\frac{a(r) - 1}{r}\right)\varepsilon_{ijk}\sigma_j\hat{x}_k , \quad n_i = \hat{x}_i \quad f = f(r) . \tag{4}$$

The static Hamiltonian reduces to the one dimensional energy density functional

$$H = 4(a')^2 \quad + \quad \frac{2(a^2 - 1)^2}{r^2} + \frac{1}{2}[r^2(f')^2 + 2a^2\sin^2 f]$$

$$+ \quad 4\kappa a^2\sin^2 f\left[(f')^2 + a^2\frac{\sin^2 f}{2r^2}\right] + \lambda(1 - \cos f)r^2 , \tag{5}$$

whose equations of motion are to be solved subject to the asymptotic conditions

$$\lim_{r\to 0} f(r) = \pi , \qquad \lim_{r\to\infty} f(r) = 0 , \tag{6}$$

$$\lim_{r\to 0} a(r) = 1 , \qquad \lim_{r\to\infty} a(r) = \pm 1 . \tag{7}$$

Recall that in the $\lambda = 0$ case in [1, 2], the boundary values (7) are instead

$$\lim_{r\to 0} a(r) = 1 , \qquad \lim_{r\to\infty} a(r) = 0, \pm 1 . \tag{8}$$

---

[1]Other potentials can also be employed if exponential localisation is not insisted on. In particular for solitons with nonvanishing magnetic flux [4] exponential localisation is not obtained with the pion-mass potential

The asymptotic values (6) of the function $f(r)$ are consistent with analyticity at the origin and finite energy at infinity. The latter condition is ensured by the presence of the pion mass potential (3). This contrasts with the ungauged model (resulting from putting $a(r) = 1$ in (5)) for which the asymptotic condition (??) follows from the finite energy condition whether or not $\lambda = 0$. If in the gauged model one puts $\lambda = 0$, then condition (6) can be imposed as a constraint for *unit* Baryon charge, so that the solutions studied in [1, 2] are constrained solutions..

Concerning the asymptotics of the function $a(r)$, the first member of (7) ensures differentiability at the origin, but the second member does not follow from the requirement of finite energy by a naive inspection of the functional (5). Doing the latter would yield instead the weaker condition

$$\lim_{r \to \infty} a' = 0 \quad \Rightarrow \quad \lim_{r \to \infty} a = a_0 \in \mathbf{R} \tag{9}$$

fixing only the r derivative of $a(r)$ at infinity. The second members of (7) and (8), result from a careful asymptotic analysis of the second order equations of motion to be given in Section 2. The results of the numerical analysis will be reported in Section 3, and summarised in Section 4.

2   Asymptotic analysis: dominant balance

The Euler-Lagrange equations for (5) are

$$(r^2 + 8\kappa a^2 \sin^2 f)f'' + 2rf' + 16\kappa aa' \sin^2 ff' + 8\kappa a^2 \sin f \cos f(f')^2$$
$$-2a^2 \sin f \cos f - 8\kappa \frac{a^4 \sin^3 f \cos f}{r^2} - \lambda r^2 \sin f \;=\; 0 \;, \tag{10}$$

$$a'' + \frac{a(1 - a^2)}{r^2} - \frac{1}{4}a \sin^2 f - \kappa a \sin^2 f(f')^2 - \kappa \frac{a^3 \sin^4 f}{r^2} \;=\; 0 \;, \tag{11}$$

and the following boundary conditions are imposed:

$$f \to 0, \quad a \to a_0 \in \mathbf{R}, \quad f' \to 0, \quad a' \to 0 \quad \text{as } r \to \infty \;. \tag{12}$$

We want to show that there are no solutions to the differential equations (10)-(11) in the asymptotic region if $a_0 = \pm 1$ is not satisfied. The $\lambda \neq 0$ case of interest here differs from the case where $\lambda = 0$. First, here we will find exponential rather than power decay of the function f. Second, the asymptotic behaviour not ruled out by the asymptotic analysis presented here is $a_0 = \pm 1$, whereas in the case $\lambda = 0$ it is $a_0 = 0, \pm 1$. The numerical results are, of course, in accordance with the asymptotic analysis.

To identify the dominant terms in the asymptotic region we use that

$$8\kappa a^2 \sin^2 ff'' \ll r^2 f'', \quad 16\kappa aa' \sin^2 ff' \ll 2rf',$$

$$8\kappa a^2 \sin f \cos f(f')^2 \ll 2rf', \quad 8\kappa \frac{a^4 \sin^3 f \cos f}{r^2} \ll 2a^2 \sin f \cos f \ll \lambda r^2 \sin f \;.$$

3

Therefore to leading order (10) reduces to

$$r^2 f'' + 2r f' - \lambda r^2 f = 0 \; , \tag{13}$$

which can be solved in terms of Bessel functions. The asymptotic behaviour of the solution is

$$f \approx \frac{f_0}{r} \exp(-\sqrt{\lambda} r) \; . \tag{14}$$

Note that in the case $\lambda = 0$, equating the terms of leading order in (10) yields

$$r^2 f'' + 2r f' - 2a_0^2 f = 0 \; . \tag{15}$$

This equation has

$$f = f_0 r^{-(1+\sqrt{1+8a_0^2})/2} \tag{16}$$

as a family of solutions which satisfies the boundary condition for f.

In the asymptotic region we also have

$$\kappa a \sin^2 f (f')^2 \ll \frac{1}{4} a \sin^2 f, \quad \kappa \frac{a^3 \sin^4 f}{r^2} \ll \frac{1}{4} a \sin^2 f \; .$$

In terms of $A = a - a_0$ we therefore obtain from (11) to leading order

$$r^2 A'' + (1 - 3a_0^2) A = a_0 (a_0^2 - 1) + \frac{r^2}{4} (a_0 + A) f^2 \; . \tag{17}$$

Because of the exponential decay of f in the case $\lambda \neq 0$, the equation reduces to

$$r^2 A'' + (1 - 3a_0^2) A = a_0 (a_0^2 - 1) \; . \tag{18}$$

For $3a_0^2 = 1$ the general solution of (18) is

$$A = \frac{2}{3\sqrt{3}} \log r + c_1 + c_2 r \tag{19}$$

which does not go to zero and is unacceptable. The solutions of (18) for $|a_0| < \frac{1}{2}$, $a_0 = \pm \frac{1}{2}$ and $|a_0| > \frac{1}{2}$ are, respectively,

$$A = \frac{a_0^3 - a_0}{1 - 3a_0^2} + \sqrt{r} \left[c_3 \cos(\frac{1}{2}\sqrt{3 - 12a_0^2} \log r) + c_4 \sin(\frac{1}{2}\sqrt{3 - 12a_0^2} \log r) \right] \; , \tag{20}$$

$$A = \mp \frac{3}{2} + c_5 \sqrt{r} + c_6 \sqrt{r} \log r \; , \tag{21}$$

$$A = \frac{a_0^3 - a_0}{1 - 3a_0^2} + \sqrt{r} \left(c_7 r^{\sqrt{12a_0^2 - 3}/2} + c_8 r^{-\sqrt{12a_0^2 - 3}/2} \right) \; , \tag{22}$$

which for $a_0 \neq \pm 1$ do not go to zero either. So there is no solution of the equation (11) for which $a_0 \neq \pm 1$. Equation (18) has solutions with acceptable asymptotic

4

behaviour only if $a_0 = \pm 1$, given by (22). In this case $A \approx c_8 r^{-1}$ (with $c_7 = 0$)is a solution with acceptable behaviour in the asymptotic region.

The situation here should be contrasted with the case where $\lambda = 0$. There [1], for $a_0 = 0$,

$$f \approx \frac{f_0}{r}, \quad A \approx A_0 r^{(1-\sqrt{f_0^2-3})/2} \tag{23}$$

is an acceptable solution of (15) and (17) in the asymptotic region if $|f_0| > 2$. In all cases the existence of acceptable solutions for small and large r of course does not guarantee the existence of a solution which has both, acceptable behaviour for small and for large r.

3   Numerical results

Before presenting our numerical results for the $\lambda \neq 0$ case, let us recall those for the system (5) with $\lambda = 0$, carried out in [1, 2]. With respect to the Skyrme coupling constant κ, only two energy branches of stable solutions were found. These are presented in Figure 1 and labelled A and B respectively. The branch A corresponding to $a(\infty) = 1$ starts from $\kappa = 0$ and persits up to a cusp critical point κ_1^{cr}. The classical energy is an increasing function of κ (with $E(\kappa = 0) = 0$). Branch B corresponding to $a(\infty) = 0$ starts from another critical point κ_2^{cr} and persists up to $\kappa \to \infty$. Branches A and B are bridged by a branch A' which like A has $a(\infty) = 1$ and is known to be unstable [5]; the numerical values $\kappa_1^{cr} \approx 0.8091$, $\kappa_2^{cr} \approx 0.6914$ were found in [2]. No solutions with $a(\infty) = -1$ were found, for which we do not have an explanation.

As we have no explanation for our inability to construct solutions with $a(\infty) = -1$ for the $\lambda = 0$ system, we have used a different numerical procedure as well as the alternative ways to implement the boundary conditions to attempt to construct them and/or to recover the results of [1, 2]. Namely, this involves the use of the boundary values (6) for the chiral function $f(r)$, while for the gauge function $a(r)$ we have used the first member of (7) together with (9). In this way, we indeed recovered the branches A, A' and B found in [1, 2] but nothing else. This provides a good check on the correctness of the numerical procedure to be applied to the $\lambda \neq 0$ system in the present work.

After all these tests involving the boundary condition (9) we have applied our numerical routines to the $\lambda \neq 0$ system and we now discuss the results. Various types of solutions are presented below for the value of $\lambda = 1.0$ but we have checked that for generic values of this parameter, the corresponding solutions display the same qualitative features .

First, the numerical analysis confirms the occurence of a branch of solutions obeying $a(0) = a(\infty) = 1$. It exists for all values of κ and the energy increases monotonically with this parameter, as illustrated on Fig. 2 (branch A). This solution can further be characterized by x_m, the value of x where $a(x)$ attains its local minimum. The following results hold :

$$\lim_{\kappa \to 0} x_m = 0 \quad , \quad \lim_{\kappa \to \infty} x_m \equiv \tilde{x}_m \approx 1.33. \tag{24}$$

For sufficiently high values of κ, our numerical analysis also reveals the existence of two branches of solutions obeying $a(0) = -a(\infty) = 1$. For instance, for $\kappa > \kappa_c$ ($\kappa_c \approx 2.297$ in the case $\lambda = 1$), we constructed two different branches of solutions, labelled C an C' on Fig. 2. As indicated the classical energies of these solutions are slightly higher than the corresponding one on branch A. In the limit $\kappa \to \kappa_c$, the two branches C and C' coincide.

We also find (using obvious notations $E_A =$ energy on branch A,...)

$$\lim_{\kappa \to \infty}(E_C - E_A) = 0 \ . \tag{25}$$

The two new solutions can further be characterized by the value x_0 where the function $a(x)$ takes its (unique, as far as we can see) node. The evolution of x_0 as a function of κ for the two branches is displayed on Fig. 3; this figure clearly indicates that, for κ fixed, the two solutions are distinguished by the position of their node. The numerical results suggest that

$$\lim_{\kappa \to \infty} x_0 = \lim_{\kappa \to \infty} x_m = \tilde{x}_m \quad \text{for branch C} \ , \tag{26}$$

$$\lim_{\kappa \to \infty} x_m = \infty \quad \text{for branch C}' \ , \tag{27}$$

Finally, on Fig. 4, the profiles of $a(x)$ for different values of κ and on the different branches are compared. It is seen that, on the interval $[0, x_m]$, the function $a(x)$ corresponding to the solutions C and C' deviates only a little from the corresponding one on branch A. The differences between the three solutions are rather perceptible on the interval $[x_m, \infty]$.

Quantitatively the value of λ affects the value of κ_c slightly. We find numerically $\kappa_c = 2.423$, 2.359 , 2.297 respectively, for $\lambda = 0.1$, 0.5 , 1.00. For all cases, we checked that the profiles of $a(x)$ and of $f(x)$ obey the asymptotic behaviours obtained in the previous section, providing a nice check of our numerics. The various solutions were obtained by using the subroutine COLSYS [6] (based on the damped Newton method of quasi-linearization, a brief description of it is presented in the Appendix of [7]). The solutions were obtained with a high degree of accuracy : typically with errors less than 10^{-8}.

The solutions displayed by Fig. 2, constitute the main result of the present work. Comparison of Figs. 2 and 1 shows that the inclusion of the pion-mass potential in the gauged sigma model has a considerable qualitative effect compared to the case when this potential is absent.

Concerning the stability of the pattern of solutions displayed in Fig. 2, we have not carried out a detailed quantitative analysis. However we beleive that the solutions on the branches A, C and C' possess respectively zero, one and two unstable modes. The stability of branch A is guaranteed by the toplogical lower bound associated with the nontrivial asymptotics of the Skyrme field. The plot of the energy corresponding to the branches C, C' terminates into a cusp, typical of catastrophe theory (see e.g. [8]). In such situations it is believed (and it was demonstrated numerically in a particular case [9]) that the number of negative modes of the upper branch of the cusp exceed

by one unit the number of negative modes of the lower branch. With our expectation of the number of unstable modes, the calculation of the Morse index

$$\xi \equiv \sum_q (-1)^q N_q \qquad (28)$$

(the sum runs over the classical solutions, q counts the number of negative modes of the solution and N_q represents the number of them) leads to $\xi = 1$ irrespectively of the parameter κ.

4   Summary

We have investigated the effect of adding the pion mass-potential, namely the last term in (5), to the Skyrme model. This potential enforces the conventional asymptotic values (6) of the chiral function $f(r)$, but in the gauge-decoupled case, with $a(r) = 1$ (5), (6) is independently guaranteed by the finite energy condition. Not surprisingly in that case [3], with $a(r) = 1$, switching λ on or off results in no appreciable qualitative change in the Skyrme soliton. The power dacay for the $\lambda = 0$ case is replaced by an exponential decay in the $\lambda \neq 0$ case.

The situation is quite different in the gauged case, where the potential is necessary to have (6). On the other hand imposition of (6) also guarantees *unit* Baryon charge, hence it is tantamount to insisting on *unit* Baryon charge even if $\lambda = 0$ in (5). This is because the Baryon charge density ϱ_{top}, is a topological charge density and hence essentially a total divergence. Thus if one sought conditional solutions restricted to *unit* Baryon number by adding the density $\xi \varrho_{top}$ to the static Hamiltonian, with ξ the Lagrange multiplier, then the Euler-Lagrange equations would remain unchanged, justifying the integration of these subject to (6) without it being necessary to have $\lambda \neq 0$ in (5). The $\lambda = 0$ case was the problem analysed in [1, 2], and the solutions constructed there must be considered to be *conditional* solutions. Here we have studied the case woth $\lambda \neq 0$, and found that switching λ on results in considerable qualitative effects on the (gauged) Skyrme soliton.

This is not a surprising result, but nor is it predictable. In the present case $\lambda \neq 0$ with asymptotics (7), it was possible to construct solutions numerically with both asymptotic values $a(\infty) = \pm 1$. By contrast in the $\lambda = 0$ case with asymptotics (8), it turned out [1, 2] that out of the three possible asymptotic values (8) only for the two, $a(\infty) = 0$ and 1, could solutions be constructed numerically. Moreover, the respective energy profiles of these solutions are quite different as seen from Figs. 1 and 2.

Concerning the phyical relevance of these solitons, first we note thay they describe the low energy properties of the Nucleons [10], and then note that the $SO(3)$ gauging of this system is a perfectly natural step in the direction of the studying the effects of the $SO(3) \times SO(2)$ Standard Model on the Nucleons.

References

[1] Y. Brihaye and D.H. Tchrakian, Nonlinearity **11** (1998) 891.

[2] Y. Brihaye, B. Kleihaus and D.H. Tchrakian, J. Math. Phys. **40** (1999) 1136-1152 [hep-th/9805059]

[3] T.H.R. Skyrme, Proc. Roy. Soc. **A 260** (1961) 127; Nucl. Phys. **31** (1962) 556.

[4] Y. Brihaye, B. Hartmann and D.H. Tchrakian, J. Math. Phys. **42** (2001) 3270 [hep-th/0010152]

[5] B. Kleihaus, D.H. Tchrakian and F. Zimmerschied, J. Math. Phys. **41** (2000) 816 [hep-th/9907035]

[6] U. Asher, J. Christiansen and R. D. Russel, Math. Comput. 33 (1979) 659; ACM Trans. Math. Softw. 7 (1981) 209.

[7] Y. Brihaye, B. Hartmann and J. Kunz, Phys. Rev. D62 (2000) 044008.

[8] F. V. Kusmartsev, Phys. Rep. **C183** (1989) 1.

[9] Y. Brihaye, J. Kunz and C. Semay, Phys. Rev. D42 (1990 2846.

[10] G.S. Adkins, C.R. Nappi and E. Witten, Nucl. Phys. B **228** (1983) 552.

Figure Captions

Figure 1 Energy versus κ for $a(\infty) = 1$ solutions (branches A, A') and for $a(\infty) = 0$ solutions (branch B), for (for $\lambda = 0.0$).

Figure 2 Energy versus κ for the $a(\infty) = 1$ solution (branch A) and for the $a(\infty) = -1$ solutions (branches C,C') (for $\lambda = 1.0$).

Figure 3 The evolution of the position of the node of the function $a(x)$ as a function of κ for the branches C and C'.

Figure 4 The profiles of $a(x)$ for the three solutions available for $\kappa = 2.5$ are presented : C in solid line, C' in short-dashed line, A in dot-dashed line. The profiles of $a(x)$ at the critical value ($\kappa \approx 2.3$) and for $\kappa = 2.5$ on branch C' are supplemented respectively on the long-dashed and dotted lines.
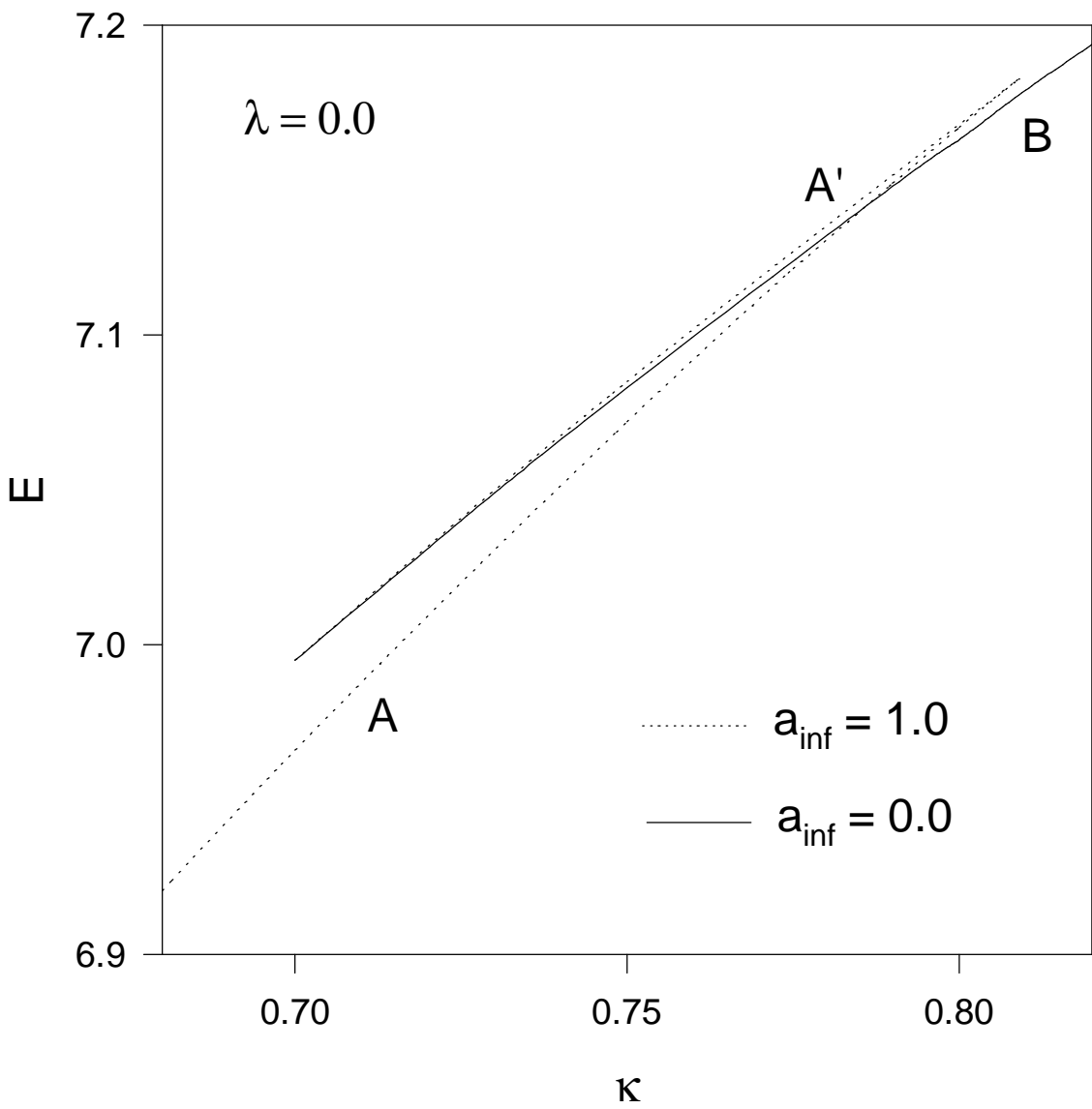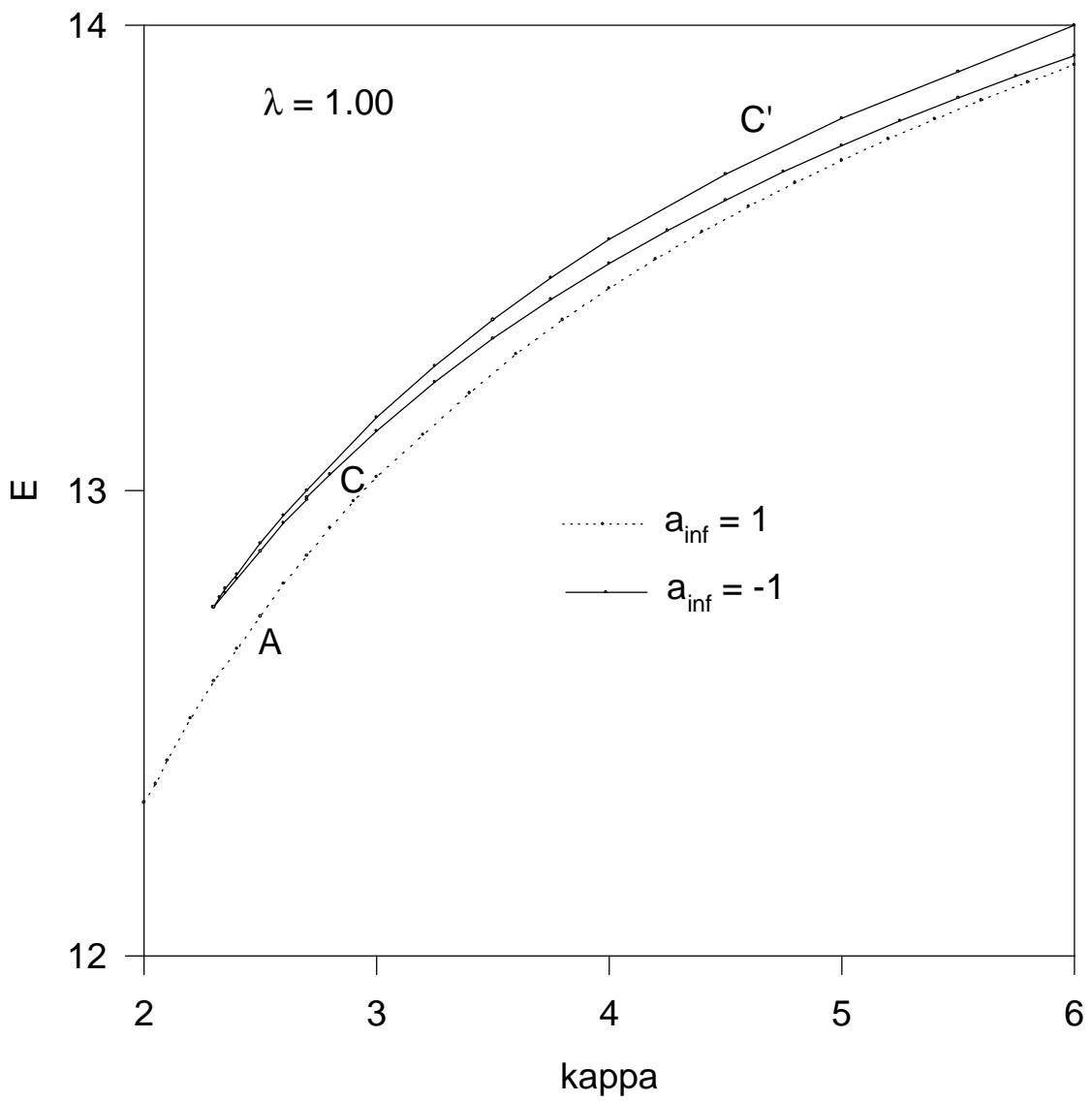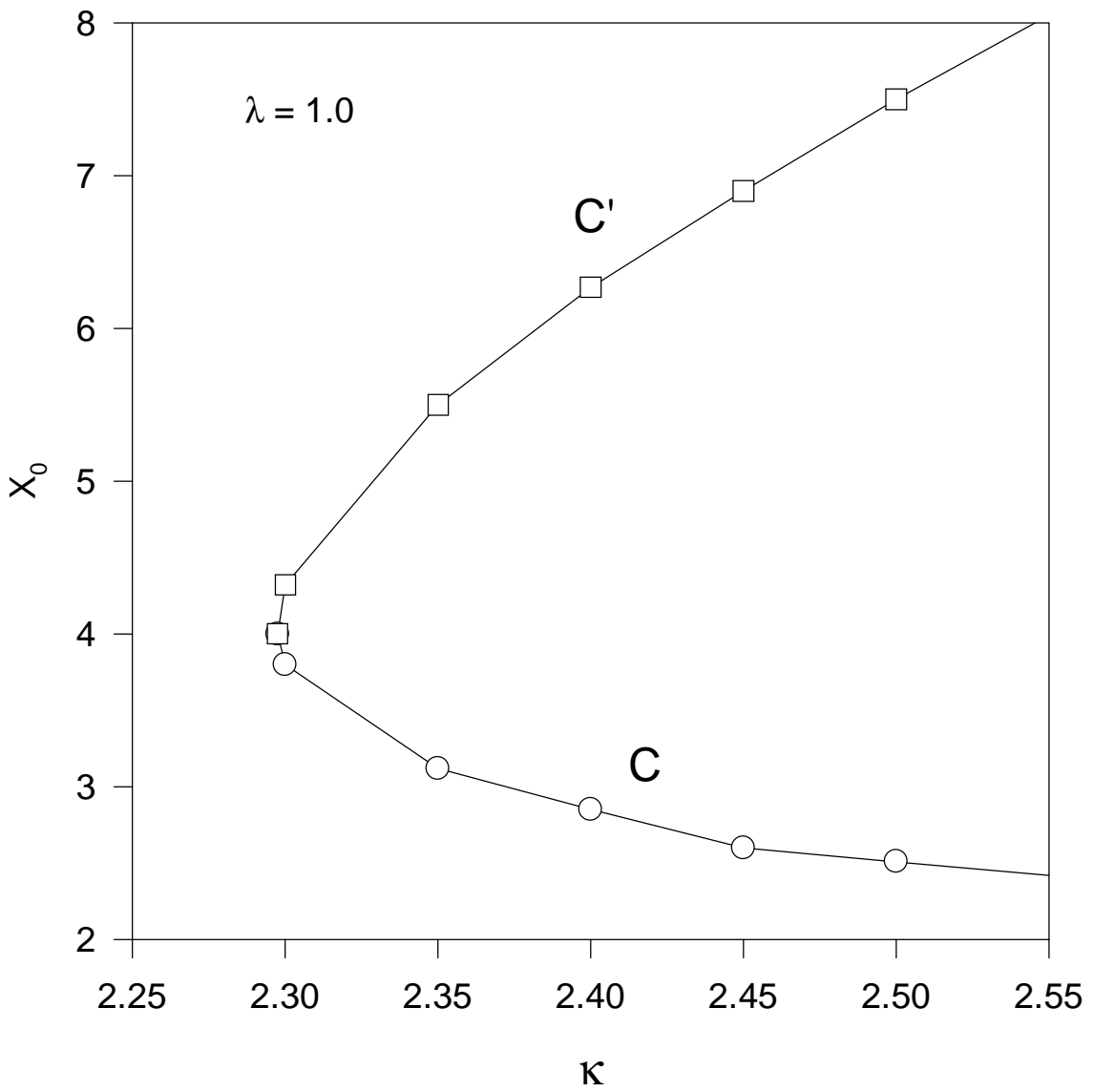
Figure 1

Figure 2

Figure 3

Figure 4